analytical chemistry

Article

Cite This: Anal. Chem. XXXX, XXX, XXX−XXX

pubs.acs.org/ac

Improved Size Determination by Nanoparticle Tracking Analysis: Influence of Recognition Radius

Ahram Kim,[†] William Bernt,[‡] and Nam-Joon Cho*[,†,§,∥]

[†]School of Materials Science and Engineering, Nanyang Technological University, 50 Nanyang Avenue 639798, Singapore

[‡]Particle Characterization Laboratories, Inc., 845 Olive Ave, Suite A, Novato, California 94945, United States

[§]Centre for Biomimetic Sensor Science, Nanyang Technological University, 50 Nanyang Drive 637553, Singapore

[∥]School of Chemical and Biomedical Engineering, Nanyang Technological University, 62 Nanyang Drive 637459, Singapore

Supporting Information

ABSTRACT: Nanoparticle tracking analysis (NTA) is a light scattering technique that measures the size distribution of suspended nanoparticles. A key parameter in NTA measurements is the recognition radius, which distinguishes individual, tracked particles from one another. However, by defining a finite radius, the displacement of tracked particles is effectively restricted, translating into an overestimation of particle size. Herein, we introduce a modified probability model that describes the restricted displacement of a tracked particle and enables more accurate nanoparticle size determination. The analytical performance of the modified displacement probability was validated through computational simulations and experimental measurements. While conventional models typically overestimated nanoparticle size by over 20%, the modified probability model estimated nanoparticle size with an error of less than 6%. The modified probability model is compatible with conventional NTA measurement readouts and thus should find wide application for more accurately determining the size distribution of suspended nanoparticles.

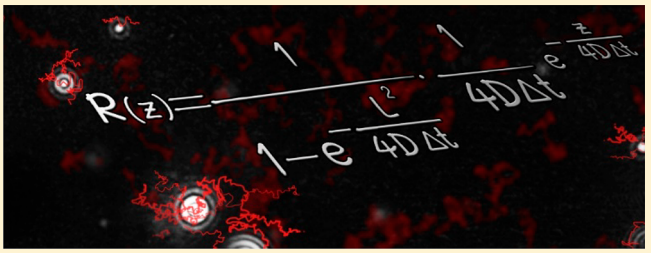

Downloaded by NANYANG TECHNOLOGICAL UNIV at 21:07:05:152 on July 02, 2019
from https://pubs.acs.org/doi/10.1021/acs.analchem.9b00454.

There is broad interest in developing analytical methods to characterize the size distribution of suspended nanoparticles for a wide range of applications such as fundamental nanoscience,[1−3] drug delivery,[4−6] toxicology,[7,8] exosomes/microvesicles,[9,10] and viral vectors.[11,12] Conventionally, dynamic light scattering (DLS) has been used to measure the ensemble-averaged size distribution of suspended nanoparticles.[13−18] However, particle size-dependent light scattering properties can affect DLS measurement accuracy for polydisperse samples.[13,16,19−22] As such, the development of highly parallel measurement techniques for characterizing individual nanoparticles is highly sought after, and nanoparticle tracking analysis (NTA) is a recently developed, light scattering-based technique that measures the size of individual nanoparticles in bulk solution.[23,24] To do so, NTA measurement captures time-lapsed, two-dimensional images of the light scattered by individual, suspended particles, computes the displacement distance of each tracked particle (particles that are visible for a certain duration across a user-defined minimum number of frames, or so-called track length), and calculates the diffusion coefficient, and hence the hydrodynamic size, of each tracked particle (Figure 1 and Supporting Information (SI) Figure S1).[23,25] Importantly, Filipe et al. showed that NTA performs similarly as well as DLS for monodisperse samples while yielding improved results for polydisperse samples.[25]

Particular attention has been placed on evaluating NTA measurement accuracy with respect to the track length or the number of frames over which a particle is tracked.[26−29] It has been shown that the uncertainty of the NTA-measured particle size is inversely proportional to the square root of the track length,[26,28,30−32] and thus a minimum track length must be considered for measurement accuracy. At the same time, an infinitely long track length is also impractical, especially when the particle concentration of a sample is high.[27,31,32] Thus, a finite track length needs to be considered for determining the size distribution, which has prompted some researchers to describe particle size distributions based on the maximum likelihood estimation (MLE) principle.[31,32] This method fits a size distribution that maximizes the likelihood of representing the acquired tracks by either an iterative approach[31] or parameter optimization.[32] In such cases, it is assumed that the two-dimensional displacements of tracked particles can be described by a Rayleigh distribution, which is the conventional distribution for Brownian motion in two dimensions.

While the Rayleigh distribution treats particle displacement as potentially infinite, the displacement of an NTA-tracked particle is bounded by the recognition radius (also known as

Received: January 25, 2019
Accepted: June 3, 2019
Published: June 3, 2019

© XXXX American Chemical Society

DOI: 10.1021/acs.analchem.9b00454
Anal. Chem. XXXX, XXX, XXX−XXX

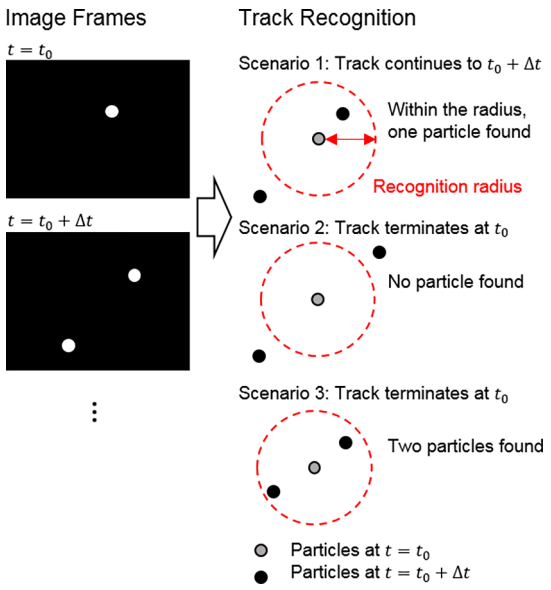

Figure 1. Schematic illustration of the NTA tracking process. One nanoparticle is detected at the initial time, t_0. At a later time point, $t_0 + \Delta t$, two nanoparticles are detected. Scenario 1: Only one nanoparticle detected at $t_0 + \Delta t$ is within the recognition radius of the nanoparticle detected at t_0. Thus, it is considered to be the same nanoparticle and nanoparticle tracking continues. Scenario 2: At $t_0 + \Delta t$, neither of the two nanoparticles is found within the recognition radius of the nanoparticle detected at t_0. Tracking of that nanoparticle is stopped at t_0. Scenario 3: Both nanoparticles detected at $t_0 + \Delta t$ are within the recognition radius of the nanoparticle detected at t_0. Thus, the nanoparticle identity at $t_0 + \Delta t$ cannot be determined and tracking of the nanoparticle is stopped at t_0.

Max Jump Distance in some commercial software packages) and rejects tracked particle displacements that exceed the recognition radius.[27,30] As a result, the NTA-measured displacement of particles is effectively reduced from its ideal displacement distribution, thereby affecting measurement accuracy.[27,33] van der Meeren et al. investigated the effect of the recognition radius on NTA measurement results using latex nanoparticle samples and observed an overestimation of the measured size when using a small recognition radius.[27] It was suggested that a recognition radius of more than three times the diffusion length is required for accurate size determination since the displacements of 99% of the tracked particles would be then within the tracking range.[27,34] However, such measurement strategies can be difficult to implement when working with relatively high particle concentrations. Moreover, when the internanoparticle distance is not sufficiently long with respect to the diffusion length of the particles, erroneous tracks can arise whereby a neighboring particle is recognized as the tracked particle.[27] For these reasons, it is important to systematically investigate how the magnitude of the recognition radius affects NTA measurement outcomes and to develop robust corrective approaches to improve NTA measurement accuracy.

Herein, we introduce a modified displacement probability that reflects the finite recognition radius for improved size distribution determination by NTA measurements. Using the modified probability model, we investigated the effect of the finite recognition radius on measurement accuracy for determining nanoparticle size distributions. Our method is based on an iterative MLE approach and incorporates the modified displacement probability into the likelihood calculation.[31] Through computational simulations and experimental measurements, we systematically evaluated the analytical performance of this modified probability model and demonstrated its measurement superiority to conventional probability models.

THEORY

Modification of Displacement Probability. To determine the size distribution of measured particles in NTA experiments, the average squared displacement of tracks is translated into particle size information based on the Stokes–Einstein equation.[23,25,26] In doing so, the average squared displacement $\langle z \rangle$ is converted into the corresponding diffusion coefficient, D, which is expressed as

$$\langle z \rangle = 4D\Delta t \tag{1}$$

where Δt is the time interval between frames. The relation is derived from the displacement probability describing the Brownian motion, which is expressed by the Rayleigh distribution, or a gamma distribution with shape K and scale u^2/K for the squared displacement z of a track consisting of K segments, where $u = \sqrt{4D\Delta t}$.[27,31,32,34] However, this relation assumes that the displacement is unbounded, meaning that the recognition radius is infinite. For a finite recognition radius, the distribution for the displacement should be modified to reflect the finite recognition radius (see SI for details). The modified displacement distribution probability relates the diffusion coefficient to the average squared displacement as follows:

$$\langle z \rangle = u^2 - L^2\left(\frac{1}{\alpha} - 1\right) \tag{2}$$

where L is the recognition radius and $\alpha = 1 - \exp(-L^2/u^2)$. The relation also predicts an overestimation of the size by the conventional probability with respect to that of the modified probability:

$$\frac{d_{\mathrm{conv}}}{d} = \frac{1}{1 - L^2/u^2\left(\frac{1}{\alpha} - 1\right)} \tag{3}$$

MATERIALS AND METHODS

NTA Simulations. A three-dimensional space was created with its width and height corresponding to the field-of-view of the CMOS camera, that is, 640 and 480 pixels, respectively.[33,35] To allow fluctuations in the number of particles detected within the field-of-view over time, an additional space that extends in each of the three dimensions was given. The extension in each direction was six times the diffusion length of the mean particle size in the simulations or at least 2 μm, and the boundary of the space was made periodic in each direction.[36] The number of generated particles was determined by the volume of the created space and the nominal particle concentration. For instance, the average number of particles observed in a frame was about 70 when the concentration was set to 1×10^9 particles/mL. The initial positions of the generated particles were assigned randomly in the three-dimensional space, and the movement of each particle in each direction in subsequent frames was randomly generated to follow a normal distribution with a standard deviation of $\sqrt{2D_i\Delta t}$,[37] where D_i is the diffusion coefficient of the ith particle and Δt was the time interval between the frames set as

DOI: 10.1021/acs.analchem.9b00454
Anal. Chem. XXXX, XXX, XXX−XXX

30.74 ms. The time duration of each simulation was 60 s, which corresponded to 1952 frames including the initial frame. The simulation did not consider either the effect of measurement errors in determining the positions of the particles or drift in the solution.[31] For the recognition of tracks, the position of a particle generated by the simulation in one frame was evaluated with respect to the position of the particles in the following frame.[27,34]

Method for Size Distribution Determination. Briefly, NTA determines the size of tracked particles from their diffusion coefficient that is acquired from the average squared displacements of the tracks. In this study, we used the maximum likelihood estimation (MLE) principle to find a size distribution that maximizes the likelihood of the obtained tracks.[31,32] In particular, an iteration-based MLE method was chosen that increases the likelihood at each iteration since it does not require prior knowledge about the particle size distribution for the iteration.[31,34,38] For a given displacement probability $P(z_m \mid n_m, d_b)$, where z_m and n_m are the average squared displacement and the track length of the mth track, respectively, and d_b is the particle size corresponding to the bth bin number of the size distribution $f(d)$, the size distribution after the rth iteration $f^{(r)}(d)$ is given by the following relation:[31,34]

$$f^{(r+1)}(d_b) = f^{(r)}(d_b)\cdot\frac{1}{M}\sum_{m=1}^{M}\frac{P(z_m|n_m, d_b)}{\sum_{b=1}^{B}P(z_m|n_m, d_b)f(d_b)/\sum_{b=1}^{B}f(d_b)} \quad (4)$$

where M is the number of observed tracks.

Both the conventional and the modified displacement probability models were used and the results were compared for the size distribution determination. A uniform size distribution was used for the initial size distribution $f^{(0)}(d)$ for both probabilities,[31,39] and the iteration terminated when the change in χ^2 became less than 1% of the value at the previous iteration.[31,34]

RESULTS AND DISCUSSION

Simulated NTA Measurements: Effects of Recognition Radius. We tested the effects of recognition radius on simulated NTA measurements by generating a model particle set with a uniform size of 100 nm and a concentration of 1×10^9 particles/mL. The simulation results were analyzed by acquiring particle tracks with a fixed recognition radius of 1, 1.5, 2, or 5 μm.[32] (see SI Figure S2(a) for the distributions of track length.) The acquired tracks were processed to recover a size distribution using the iteration-based MLE method with the conventional or modified displacement probability as shown in Figure 2(a) and (b). When the recognition radius was 2 and 5 μm, the obtained mean size was close to the nominal size regardless of the employed probabilities. However, when the recognition radius was short, that is, 1 and 1.5 μm, respectively, the mean size determined by the conventional probability was 152 and 107 nm, or an overestimation by a factor of 1.52 and 1.07, which is close to an expected factor of 1.50 and 1.06, respectively, according to eq 3. In contrast, the acquired mean size with the modified displacement probability was 102 and 100 nm at recognition radii of 1 and 1.5 μm, respectively. The data support that the overestimation of the mean size produced by the conventional probability model can be mitigated by using the modified probability model. In addition, the relative variance or variance

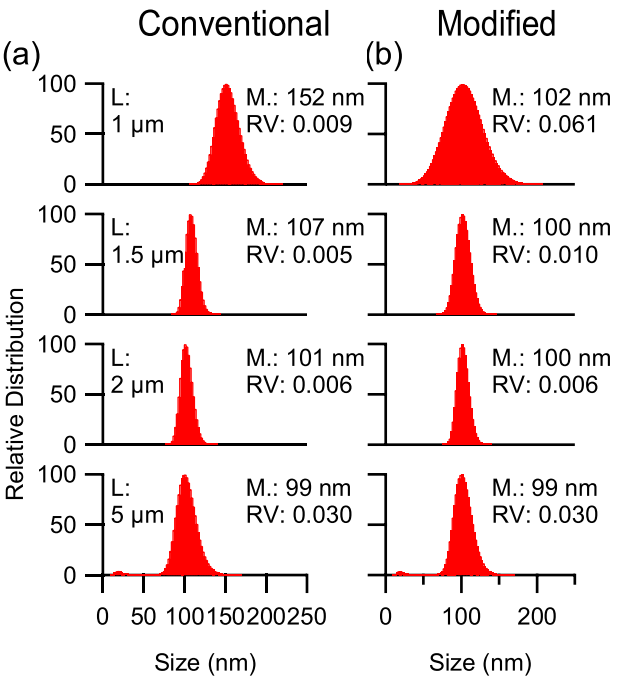

Figure 2. Simulated NTA measurements of ideally monodisperse, 100 nm diameter nanoparticles. Different recognition radius values, L, of 1, 1.5, 2, and 5 μm were tested based on a total of 8310, 5329, 4616, and 3585 tracks, respectively. Acquired tracks were processed to determine the size distribution using the iteration-based MLE method with the (a) conventional displacement probability or (b) modified displacement probability. The nanoparticle concentration was 1×10^9/mL. The computed mean diameter and relative variation (RV) for each size distribution are reported.

of the distribution divided by the square of its mean size, of 0.009 acquired with the conventional probability at a recognition radius of 1 μm is close to the nominal value, that is, 0, while the modified probability reports 0.061 at the same recognition radius for this idealized case.

To compare the two probability models in a more realistic scenario, another NTA simulation was conducted with a model particle set whose size distribution follows a normal distribution with its mean size and relative variance chosen as 100 nm and 0.05, respectively, at a concentration of 1×10^9 particles/mL. (See Supproting Information for the detail on the size distribution[32] and SI Figure S2(b) for the distribution of the tracks by the track length.) The tracks were processed to determine a size distribution using the two types of displacement probability as shown in Figure 3. Like the previous results, at a recognition radius of 2 and 5 μm, the obtained mean size regardless of the employed probability was close to the nominal mean size of 100 nm. When the recognition radius was short, that is, 1 μm, the mean size determined with the conventional probability was overestimated by a factor of 1.54 which is in line with theoretical expectations, while the mean size observed with the modified probability was 107 nm. In addition, the relative variance acquired with the conventional probability model at a recognition radius of 1 μm was 0.009, which is a significant underestimation compared to the nominal value of 0.05. By contrast, the relative variance acquired with the modified probability model is 0.083, which is modestly larger than the nominal value. Together, the data indicate that the modified probability model yields more accurate information about the

DOI: 10.1021/acs.analchem.9b00454
Anal. Chem. XXXX, XXX, XXX−XXX

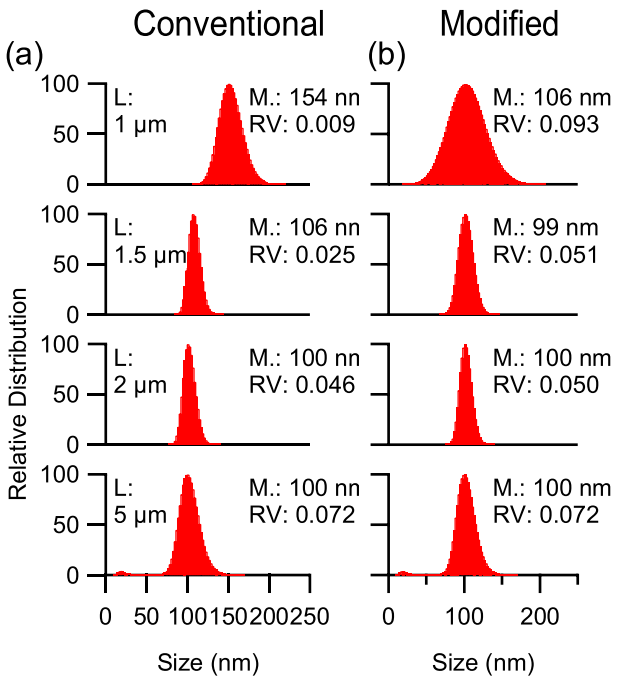

Figure 3. Simulated NTA measurements of 100 ± 5 nm diameter nanoparticles. Different recognition radius values, *L*, of 1, 1.5, 2, and 5 μm were tested based on a total of 7677, 5357, 4607, and 3564 tracks, respectively. Acquired tracks were processed to determine the size distribution using the iteration-based MLE method with the (a) conventional displacement probability or (b) modified displacement probability. The nanoparticle concentration was 1×10^9/mL. The computed mean diameter and relative variation (RV) for each size distribution are reported.

mean size and relative variation of the simulated nanoparticles in this case.

Simulated NTA Measurements: Effects of Nanoparticle Diameter. To extend the observation on the influence of the recognition radius and the displacement probabilities, a series of NTA simulations with model size distributions of various mean size and relative variance were conducted. Mean size of 20, 50, 100, and 200 nm and relative variance of 0, 0.01, and 0.05 were chosen for the model size distributions at a concentration of 1×10^9 particles/mL, where two types of particle size distributions were evaluated for each pair of mean size and relative variance: one from a normal distribution and the other from a bimodal distribution (see SI for more details). The simulated results were processed to construct tracks at various recognition radii from 1 to 5 μm and analyzed to determine the size distribution with the two displacement probabilities.

The mean size and relative variance determined from the simulations with a normal distribution and a bimodal distribution are presented in SI Figures S3 and S4, respectively. Similar trends were obtained with both distributions. The results show that the acquired mean size with the conventional probability follows the expected overestimation (dashed lines) regardless of the simulation condition, while the modified probability gives the mean size values in line with their respective nominal sizes. Again, a minimum length of the recognition radius (typically >1.5 μm) was needed to obtain more accurate results.

On the other hand, the relative variance acquired with the two probabilities shows a deviation from the nominal value when the recognition radius was very long, unlike what is observed with the mean size results. In fact, when the recognition radius is 5 μm, a spurious peak was found at a small-size range in the acquired size distributions besides the major peak centered at the nominal mean size (cf. Figures 2 and 3). It is probable that the observed spurious peak contributes to the increased relative variance at the long recognition radius values. Such spurious peaks can be produced due to false tracks made during the NTA track recognition, where two different particles are recognized as the same particle over two successive frames and form a false track which cannot be screened by the NTA tracking principle.[27] This is obvious if the simulation results are processed again when those false tracks are excluded from the analysis. SI Figures S5 and S6 show the determined size distributions acquired from the screened tracks of the previous simulations with a nominal relative variance of 0 and 0.05, respectively. From the acquired size distributions with the screened tracks, no spurious peak was found at a small size range. In addition, the relative variance acquired from the screened track data, regardless of the probability model that was applied for the analysis, is very close to the nominal value at a long recognition radius. When the exclusion of false tracks is applied to the analysis of all the simulations used in SI Figure S3, it becomes more apparent that the increased relative variance at a long recognition radius results from the false tracks, as shown in SI Figure S7. This suggests that NTA analysis can be corrupted by false tracks if too long of a recognition radius is used for track recognition.[27]

With decreasing recognition radius, the obtained relative variance decreases gradually and approaches that of their respective nominal values regardless of the displacement probability used in the analysis. This indicates that the false tracks can be reduced by decreasing the recognition radius. When the recognition radius was even smaller, the determined relative variance started to deviate from the nominal value to a very small value when analyzed with the conventional probability or to a very large value with the modified probability. Hence, to obtain accurate particle size information with the modified probability model, it is important to also select an appropriate recognition radius that is neither too short nor too long.

Simulated NTA Measurements: Size Resolution of NTA. To investigate and compare the size resolution of NTA depending on the employed probability model and recognition radius value, we evaluated the size distributions acquired from the previous simulations using a bimodal size distribution as described in SI Figure S4. Figure 4 identifies the position of the peaks found from the results of the bimodal size distribution simulations that were analyzed with the two probabilities across various recognition radii from 1 to 5 μm.

At a long recognition radius, where the recognition radius is long enough compared to the diffusion length, the two peaks are observable for the nominal mean sizes of 50, 100, and 200 nm. The identified positions agree well with their respective nominal peak positions regardless of the probability model. A spurious peak at a small-size range was also observed for the three mean size conditions at a very long recognition radius, for example, 5 μm. However, it was not possible to resolve the two separate peaks when the nominal mean size was 20 nm at the recognition radius regardless of the displacement probability.

DOI: 10.1021/acs.analchem.9b00454
Anal. Chem. XXXX, XXX, XXX−XXX

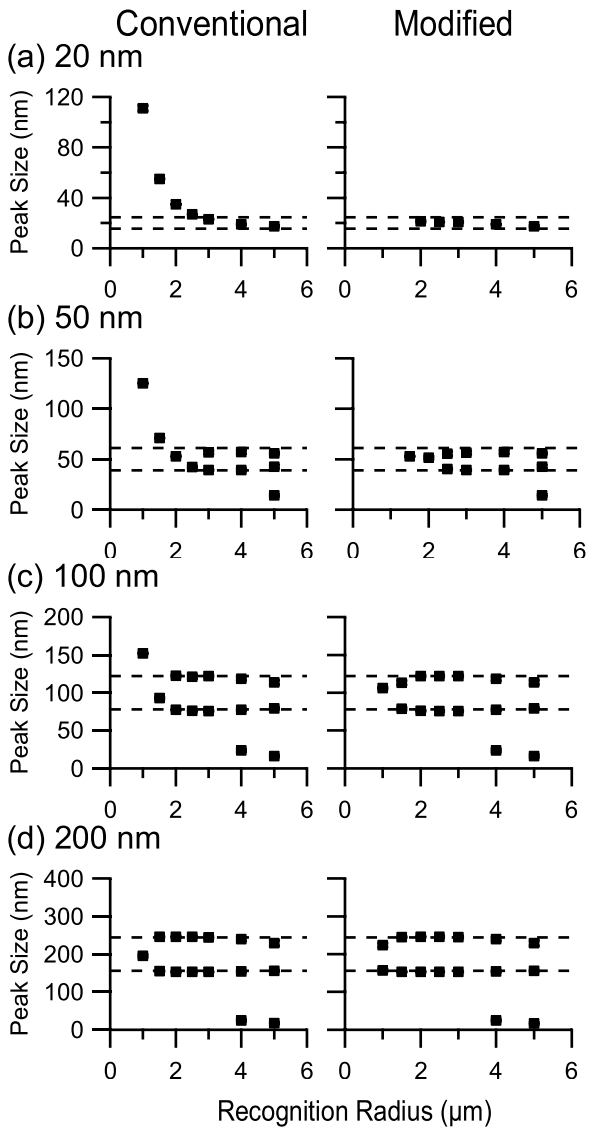

Figure 4. Simulated NTA measurements as a function of nanoparticle diameter. Nanoparticle suspensions were simulated with different mean nanoparticle diameters of (a) 20, (b) 50, (c) 100, and (d) 200 nm. The nanoparticle size distributions had an RV of 0.05, and the nanoparticle concentration was fixed at 1×10^9/mL. Acquired tracks were processed to determine the size distribution using the iteration-based MLE method with the conventional displacement probability (left) or modified displacement probability (right). The peak positions in each size distribution are plotted as black squares and the simulations were conducted with different recognition radius values. In the simulations, each nanoparticle suspension was composed of two types of nanoparticles with different sizes and mixed in equal number fractions. The 20-, 50-, 100-, and 200 nm diameter nanoparticle sets were composed of 16- and 25-, 39-, and 61-, 78,- and 122-, and 155- and 245 nm diameter nanoparticles, respectively. Dashed lines correspond to the diameters of the nanoparticles that were mixed in each sample.

At a short recognition radius regardless of the displacement probability, on the other hand, only a single peak is identified for all the mean size conditions. This confirms that a short recognition radius limits the size resolution of NTA measurements and hinders accurate distribution determination. Remarkably, the lower limit of the recognition radius to resolve the two separate peaks is lower with the modified probability than the conventional probability. This makes the modified probability more advantageous where the recognition radius should be limited, for example, in a high particle concentration condition, which gives a reduced interparticle distance.

Simulated NTA Measurements: Influence of Particle Concentration. We observed that false tracks could undermine accurate size distribution determination in NTA measurements. Since false tracks are created when two different particles are recognized as the same particle, the probability of false track creation would depend on the concentration of particles as well as the recognition radius set for the analysis.[27] Furthermore, an increase in the particle concentration would lead to a higher probability of early termination of the particle tracking process since neighboring particles around the tracked particle would more likely jump into the recognition radius zone and more frequently interrupt the tracking process.[27] This suggests that an increased particle concentration results in poorer resolution of NTA size distribution determination along with the influence of the false tracks since the uncertainty of the determined size of a track is inversely proportional to the square root of its track length.[26,28,30−32]

To evaluet the effect of particle concentration, a series of NTA simulations with a model particle set with a uniform size of 20, 50, 100, or 200 nm at various concentrations of 1×10^8, 1×10^9, and 1×10^{10} particles/mL were conducted. The acquired mean size and relative variance are presented in SI Figure S8. The dependence of the mean size on the recognition radius shows the same results as what was observed in the previous results regardless of the concentration condition, whereas the relative variance of the acquired size distributions shows a significant dependence on the concentration condition. At a higher concentration, the relative variance of the determined size distributions reports a larger value for all the nominal mean size conditions and recognition radius values. The observation indicates that the size distribution acquired with NTA reports a broader distribution than the true distribution, where the degree of the broadening increases at higher particle concentrations.

As discussed earlier, the larger relative variance at higher concentration conditions could be due to an increased number of false tracks. To investigate false tracks, the simulation results were reanalyzed with the suspected false tracks excluded from the analysis (see SI Figure S9). Overall, the two displacement probabilities provided very similar results to each other when evaluated at the recognition radius of 5 μm and at a concentration of 1×10^8 particles/mL. Since the number of particles detected in the field-of-view is very small at this specific concentration level, that is, approximately seven particles, it is unlikely that the tracking process is corrupted by false tracks and the relative variance is not much different from when the false tracks are included or excluded. On the other hand, at a concentration of 1×10^9 particles/mL, the acquired relative variance values are very similar to the corresponding relative variance values measured at the concentration of 1×10^8 particles/mL, indicating that the larger, uncorrected relative variance at the concentration of 1×10^9 particles/mL is due to false tracks.

At a concentration of 1×10^{10} particles/mL, the relative variance of the determined size distribution at the same recognition radius of 5 μm is significantly smaller than those acquired with the false tracks included, meaning that the false

DOI: 10.1021/acs.analchem.9b00454
Anal. Chem. XXXX, XXX, XXX−XXX

tracks make the acquired size distribution much broader. Nevertheless, the values are larger than their corresponding values measured at the concentration of 1×10^8 and 1×10^9 particles/mL, which indicates that false tracks are not the only source of the broad size distribution that is determined by NTA at a very high particle concentration.

Another likely cause of such a broad size distribution as measured by NTA is an early termination of tracks due to an increased number of neighboring particles at higher particle concentrations (see SI Figure S10 for the average track length of the acquired tracks at various nominal mean sizes and concentrations). The significant difference in the average track length depending on the particle concentration suggests that the reduced average track length results in a broader size distribution with increasing particle concentration.

From the observation, we could expect a narrower size distribution from NTA if we reduce the probability of the tracking termination and hence increase the average track length. This is obvious from SI Figure S8, where the relative variance becomes smaller with a decreasing recognition radius regardless of the mean size and the concentration. The observation is further supported by the average track length depending on the recognition radius as shown in SI Figure S10. This finding suggests that a smaller recognition radius would be preferred to acquire a narrower size distribution for a longer track length of the tracks used for NTA analysis, resulting in the modified probability model yielding more accurate measurement results.

Experimental Validation of the Modified Probability Model. Having tested the conventional and the modified displacement probabilities on the simulated results, we applied the two probabilities to analyze experimental NTA data. Two polystyrene (PS) latex standards of nominal mean sizes of 51.6 and 181.6 nm were measured at two different particle concentration conditions, namely 1×10^8 and 1×10^9 particles/mL. The particle tracks from NTA were constructed at various recognition radius values from 1.1 to 5.4 μm and processed with the conventional and modified displacement probabilities. Figure 5 shows the results of NTA measurements on the PS latex standards.

For the sample of a nominal mean size of 51.6 nm, the mean size obtained with the conventional probability is close to the nominal mean size at a recognition radius of 5.4 μm, as shown in Figure 5(a) and (b). At this recognition radius, the mean size obtained with the modified probability is the same as that acquired with the conventional probability. Remarkably, the slight deviation of the acquired mean size from the nominal value seems to be due to the increased relative variance which is discussed below. In fact, the modal value of the determined size distribution listed in SI Table S1 is very close to the nominal size for the two concentration conditions.[35] With a subsequent decrease in the recognition radius, the mean size acquired with the conventional probability model gradually increases. The modified probability reports a consistent mean size value regardless of the recognition radius, although it failed to acquire a proper size distribution when the recognition radius was below 1.6 μm. For the nanoparticle sample of a nominal mean size of 181.6 nm, the acquired mean size results showed the same trend as that observed with the 51.6 nm standard sample, as shown in Figure 5(c) and (d).

The relative variance acquired with the two displacement probabilities is also in line with the simulation results. For the sample of a nominal mean size of 51.6 nm, the relative

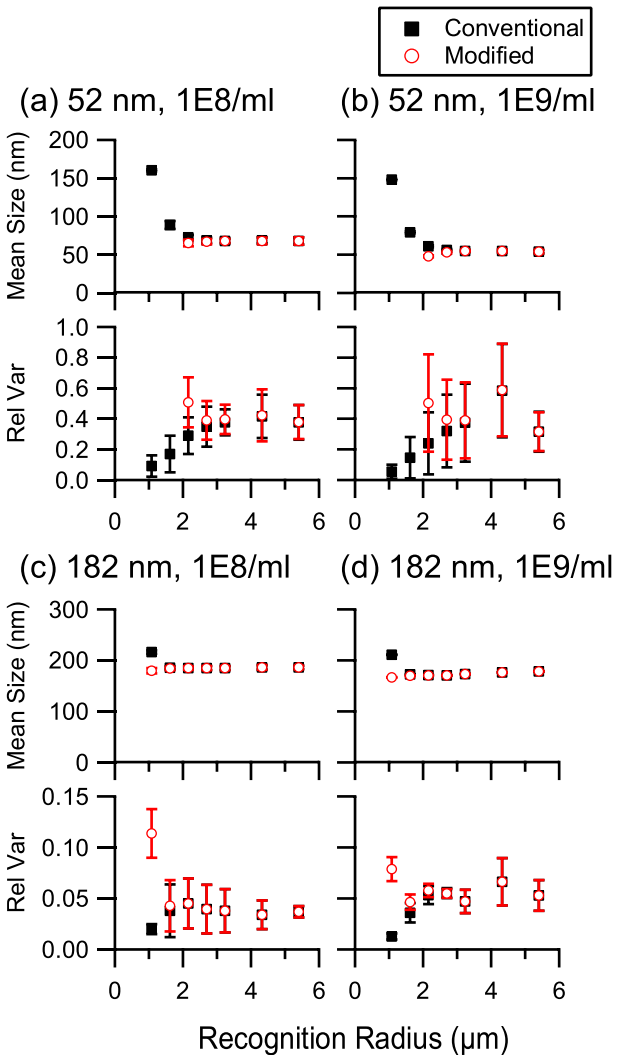

Figure 5. NTA experimental validation of the modified probability model. NTA measurements were conducted on 52 nm diameter PS latex nanoparticles at particle concentrations of (a) 1×10^8 (left) and (b) 1×10^9 particles/mL. (c,d) Similar measurements were conducted on 182 nm diameter PS latex nanoparticles. The calculated mean diameter and standard deviation (denoted as error bar; $n = 3$ measurements) for each sample are reported as a function of recognition radius value. The data points obtained using the iteration-based MLE method with the conventional displacement probability or modified displacement probability are indicated by black squares and white circles, respectively.

variances acquired with the modified probability are the same as those from the conventional probability at a recognition radius of 5.4 μm. With a decreasing recognition radius, the relative variance acquired with the conventional probability gradually decreases as is observed for the simulated results. The modified probability reports the same value compared with the conventional probability as the recognition radius decreases. When the recognition radius becomes even smaller, the relative variance acquired with the modified probability shows a value different from that acquired with the conventional probability and started to increase, as observed in the simulation results.

For the sample with a nominal mean size of 181.6 nm, the relative variance acquired with the conventional probability decreases with a decreasing recognition radius, as was seen

DOI: 10.1021/acs.analchem.9b00454
Anal. Chem. XXXX, XXX, XXX−XXX

from the smaller 51.6 nm sample as well. The relative variance acquired with the modified probability shows the same behavior, where it reports the same value as that acquired with the conventional probability with a subsequent decrease from 5.4 μm and starts to deviate from their corresponding values obtained with the conventional probability at very small recognition radius values.

Regarding the large relative variance observed at long recognition radius values, the simulation results indicate that is occurs due to false tracks, where two different particles are recognized as the same particle. Indeed, as presented in SI Figure S11, the size distribution of the 51.6 nm standard acquired at a recognition radius of 5.4 μm shows a spurious peak that is also seen in the simulation results (see SI Figure S12). However, the relative variance of the 51.6 nm standard is much larger compared to the values observed in the simulation results. This difference seems to occur due to false identification of phantom particles, thereby increasing the probability of false tracking.[29,30,40,41] Since the scattered light from the 51.6 nm particles is not strong enough to be highly distinguished compard to the background noise, artifacts might be identified as particles and thus introduce more false tracks. As a larger particle scatters more light, it is easier to be distinguished from the background and we can expect fewer false tracks and smaller relative variance. For the 181.6 nm standard, the relative variance of the size distribution acquired at a long recognition radius is significantly smaller than that observed with the 51.6 nm standard. This indicates that the size distribution of smaller particles analyzed by NTA could have higher uncertainty due to their weak scattering power that introduces more false tracks, and suggests considerations on the experimental conditions for a better size distribution measurement.

CONCLUSION

In this work, we have described an improved method for determining the NTA-measured size distribution of suspended nanoparticles based on the MLE approach. By considering the recognition radius used for particle tracking in NTA, a modified displacement probability was introduced for the likelihood calculation of the MLE method. Computational simulations and experimental measurements verified that the conventional probability model results in an overestimation of nanoparticle diameter when a short recognition radius is used, while the estimated mean size obtained with the modified probability model is negligibly affected by the recognition radius. We also discuss important technical points arising from the selection of short and long recognition radius values along with the effects of nanoparticle concentration. Taken together, our findings provide an improved method for accurately determining particle distributions in NTA measurements and these analytical capabilities should prove useful for a wide range of nanoscience and nanotechnology applications.

ASSOCIATED CONTENT

Supporting Information

The Supporting Information is available free of charge on the ACS Publications website at DOI: 10.1021/acs.analchem.9b00454.

Additional information is provided about the modified displacement probability with respect to the recognition radius, schematic diagram of the NTA principle (Figure S1), NTA simulation results (Figures S2−S10) and the size distributions acquired from NTA measurements on PS latex standard samples (Figures S11) (PDF)

AUTHOR INFORMATION

Corresponding Author

E-mail: njcho@ntu.edu.sg.

ORCID

Nam-Joon Cho: 0000-0002-8692-8955

Notes

The authors declare no competing financial interest.

ACKNOWLEDGMENTS

This work was supported by the National Research Foundation of Singapore through a Competitive Research Programme grant (NRF-CRP10-2012-07) and a Proof-of-Concept grant (NRF2015NRF-POC0001-19). Additional support was provided by the Creative Materials Discovery Program through the National Research Foundation of Korea funded by the Ministry of Science, ICT and Future Planning (NRF-2016M3D1A1024098).

REFERENCES

(1) Dong, C.; Lian, C.; Hu, S.; Deng, Z.; Gong, J.; Li, M.; Liu, H.; Xing, M.; Zhang, J. *Nat. Commun.* **2018**, *9* (1), 1252.

(2) Peng, R.; Li, S.; Sun, X.; Ren, Q.; Chen, L.; Fu, M.; Wu, J.; Ye, D. *Appl. Catal., B* **2018**, *220*, 462−470.

(3) Akamatsu, M.; Komatsu, H.; Matsuda, A.; Mori, T.; Nakanishi, W.; Sakai, H.; Hill, J. P.; Ariga, K. *Bull. Chem. Soc. Jpn.* **2017**, *90* (6), 678−683.

(4) Anselmo, A. C.; Mitragotri, S. *AAPS J.* **2015**, *17* (5), 1041−1054.

(5) Blanco, E.; Shen, H.; Ferrari, M. *Nat. Biotechnol.* **2015**, *33* (9), 941.

(6) Yingchoncharoen, P.; Kalinowski, D. S.; Richardson, D. R. *Pharmacol. Rev.* **2016**, *68* (3), 701−787.

(7) Bergin, I. L.; Wilding, L. A.; Morishita, M.; Walacavage, K.; Ault, A. P.; Axson, J. L.; Stark, D. I.; Hashway, S. A.; Capracotta, S. S.; Leroueil, P. R. *Nanotoxicology* **2016**, *10* (3), 352−360.

(8) Hofmann-Amtenbrink, M.; Grainger, D. W.; Hofmann, H. *Nanomedicine* **2015**, *11* (7), 1689−94.

(9) Caponnetto, F.; Manini, I.; Skrap, M.; Palmai-Pallag, T.; Di Loreto, C.; Beltrami, A. P.; Cesselli, D.; Ferrari, E. *Nanomedicine* **2017**, *13* (3), 1011−1020.

(10) Nguyen, D. B.; Ly, T. B. T.; Wesseling, M. C.; Hittinger, M.; Torge, A.; Devitt, A.; Perrie, Y.; Bernhardt, I. *Cell. Physiol. Biochem.* **2016**, *38* (3), 1085−1099.

(11) Riley, M.; Vermerris, W. *Nanomaterials* **2017**, *7* (5), 94.

(12) Wong, J. K.; Mohseni, R.; Hamidieh, A. A.; MacLaren, R. E.; Habib, N.; Seifalian, A. M. *Trends Biotechnol.* **2017**, *35* (5), 434−451.

(13) Pecora, R. *Dynamic Light Scattering: Applications of Photon Correlation Spectroscopy*; Springer Science & Business Media, 2013.

(14) Meurant, G. *Introduction to Dynamic Light Scattering by Macromolecules*; Elsevier, 2012.

(15) Stetefeld, J.; McKenna, S. A.; Patel, T. R. *Biophys. Rev.* **2016**, *8* (4), 409−427.

(16) Hassan, P. A.; Rana, S.; Verma, G. *Langmuir* **2015**, *31* (1), 3−12.

(17) Minton, A. P. *Anal. Biochem.* **2016**, *501*, 4−22.

(18) Zheng, T.; Bott, S.; Huo, Q. *ACS Appl. Mater. Interfaces* **2016**, *8* (33), 21585−21594.

(19) Chu, B. *Laser Light Scattering: Basic Principles and Practice*;Courier Corporation,2007.

(20) Ferré-D'Amaré, A. R.; Burley, S. K. *Structure* **1994**, *2* (5), 357−359.

(21) Elofsson, U. M.; Dejmek, P.; Paulsson, M. A. *Int. Dairy J.* **1996**, *6* (4), 343−357.

DOI: 10.1021/acs.analchem.9b00454
Anal. Chem. XXXX, XXX, XXX−XXX

(22) Hawe, A.; Hulse, W. L.; Jiskoot, W.; Forbes, R. T. *Pharm. Res.* **2011**, *28* (9), 2302−2310.
(23) Malloy, A.; Carr, B. *Part. Part. Syst. Char.* **2006**, *23* (2), 197−204.
(24) Bob Carr, P. H.; Malloy, A.; Nelson, P.; Wright, M.; Smith, J. *Eur. J. Parent. Pharm. Sci.* **2009**, *14*, 35−40.
(25) Filipe, V.; Hawe, A.; Jiskoot, W. *Pharm. Res.* **2010**, *27* (5), 796−810.
(26) Boyd, R. D.; Pichaimuthu, S. K.; Cuenat, A. *Colloids Surf., A* **2011**, *387* (1−3), 35−42.
(27) Van Der Meeren, P.; Kasinos, M.; Saveyn, H., Relevance of two-dimensional brownian motion dynamics in applying nanoparticle tracking analysis. In *Methods Mol. Biol.*, **2012**; Vol. *906*, pp 525−534.
(28) Bell, N. C.; Minelli, C.; Tompkins, J.; Stevens, M. M.; Shard, A. G. *Langmuir* **2012**, *28* (29), 10860−72.
(29) Gardiner, C.; Ferreira, Y. J.; Dragovic, R. A.; Redman, C. W.; Sargent, I. L., Extracellular vesicle sizing and enumeration by nanoparticle tracking analysis. *J. Extracell. Vesicles* **2013**, *2*.19671
(30) Gross, J.; Sayle, S.; Karow, A. R.; Bakowsky, U.; Garidel, P. *Eur. J. Pharm. Biopharm.* **2016**, *104*, 30−41.
(31) Walker, J. G. *Meas. Sci. Technol.* **2012**, *23* (6), No. 065605.
(32) Saveyn, H.; De Baets, B.; Thas, O.; Hole, P.; Smith, J.; Van der Meeren, P. *J. Colloid Interface Sci.* **2010**, *352* (2), 593−600.
(33) Zhou, C.; Krueger, A. B.; Barnard, J. G.; Qi, W.; Carpenter, J. F. *J. Pharm. Sci.* **2015**, *104* (8), 2441−2450.
(34) Wagner, T.; Lipinski, H. G.; Wiemann, M. *J. Nanopart. Res.* **2014**, *16*, 2419.
(35) Hole, P.; Sillence, K.; Hannell, C.; Maguire, C. M.; Roesslein, M.; Suarez, G.; Capracotta, S.; Magdolenova, Z.; Horev-Azaria, L.; Dybowska, A.; Cooke, L.; Haase, A.; Contal, S.; Mano, S.; Vennemann, A.; Sauvain, J. J.; Staunton, K. C.; Anguissola, S.; Luch, A.; Dusinska, M.; Korenstein, R.; Gutleb, A. C.; Wiemann, M.; Prina-Mello, A.; Riediker, M.; Wick, P. *J. Nanopart. Res.* **2013**, *15*, 2101.
(36) Ladd, A. J. *Phys. Rev. Lett.* **1993**, *70* (9), 1339.
(37) Michalet, X. *Phys. Rev. E: Stat. Phys., Plasmas, Fluids* **2010**, *82* (4), No. 041914.
(38) Kestens, V.; Bozatzidis, V.; De Temmerman, P. J.; Ramaye, Y.; Roebben, G. *J. Nanopart. Res.* **2017**, *19* (8), 271.
(39) Lucy, L. B. *Astron. J.* **1974**, *79* (6), 745−754.
(40) Bai, K.; Barnett, G. V.; Kar, S. R.; Das, T. K. *Pharm. Res.* **2017**, *34* (4), 800−808.
(41) de Temmerman, P. J.; Verleysen, E.; Lammertyn, J.; Mast, J. *J. Nanopart. Res.* **2014**, *16* (10), 17.

DOI: 10.1021/acs.analchem.9b00454
Anal. Chem. XXXX, XXX, XXX−XXX